Double Impact Orbits of Periodically Forced Impact Oscillators

C.J. Budd*& A.G. Lee†

January 1995

Abstract

We consider a periodically forced oscillator which impacts against a rigid constraint. The forcing is both sinusoidal and non-sinusoidal and is made up of a combination of the first and second harmonics of a Fourier series. A simple restitution law is used to describe the impact. This paper centres around the analysis of double–impact periodic solutions, that is motions which repeat after every second impact. Solutions for these double-impact orbits are found, including non-physical orbits and unstable orbits. Behaviour typical of nonlinear dynamical systems, such as period-doubling bifurcations are detected and grazing bifurcations, which are unique to discontinuous dynamical systems are also observed. A combination of analytical and numerical techniques are used to uncover the behaviour of the system at odd multiples of the natural frequency, where numerical experiments tell us that stable double-impact periodic solutions exist. The persistence of these stable double–impact orbits are also examined as parameters are varied. We conclude by presenting some numerical calculations of two more general cases of impacting systems.

1 Introduction

An impact oscillator comprises, in general, a driven system with components which undergo instantaneous, discontinuous, changes of motion due to impacts with each other or with another obstacle. Such systems (or related systems involving piecewise linear changes in restoring force) arise naturally in many applications such as car suspensions, gear boxes [1], suspension bridges [2] and heat exchangers [3].

The dynamics of these systems can be very complex, with both periodic and chaotic behaviour observable. Moreover, very different behaviour can be observed for the same problems as parameters vary, with high amplitude (resonant) periodic motion changing to low amplitude chaotic motion. For an engineer interested in the dynamics of an impacting process, both motions can be troublesome as the high amplitude motion leads to high wear and the chaotic motion to unpredictability.

Impact oscillators are also of interest to mathematicians. Their inherent nonlinearity makes them hard to study analytically other than in the simplest cases of single impact periodic motion.

*School of Mathematical Sciences, University of Bath, Claverton Down, Bath, BA2 7AY, U.K.
†School of Mathematics, University of Bristol, Bristol, BS8 1TW, U.K.

Furthermore, there is little existing theory for the behaviour of non-smooth dynamical systems and new generic forms of motion (such as that resulting from a grazing bifurcation [4]) have only recently been discovered.

The purpose of this paper is to investigate periodic motions of a single-degree-of-freedom, forced impact oscillator which involve two impacts per period and in particular to obtain some exact analytic descriptions of them when the frequency of the forcing is an odd multiple of the natural frequency of the oscillator without impact. These double impact motions are of interest for several reasons. Firstly, the exact solutions perturb smoothly as either the forcing frequency or other parameters describing the oscillator vary. Secondly, these perturbations are stable over a range of such parameters. Furthermore, for these parameters they describe a predictable low amplitude (and thus low wear) motion of the oscillator. We also perform some numerical experiments in Section 6 which demonstrate that closely related double impact behaviour is also seen in the periodically forced and impacting Duffing oscillator and in systems with more than one impacting component.

Some of the earliest studies of periodically forced impact oscillators were numerical and analogue computer investigations by Peterka and co-workers [5, 6, 7, 8, 9, 10, 11] with more recent work being done by Shaw and Holmes [12], Shaw [13, 14, 15], Thompson, Foale and Bishop [16, 17, 18], Nordmark [4] and Budd *et. al.* [19, 20, 21, 22]. Experimental studies of impact systems on air beds have been made in [23] and of impacting cantilever beams (which oscillate in several modes) in [24, 25]. Popp and his co-workers [26, 27, 28] have also examined these systems with respect to controlling impact oscillators. The theory describing them has also found application in studies of DC-DC switching systems [29], friction oscillators [26, 27, 30] and time-series analysis [31]. The richness of the dynamics observed in impact oscillators and their immediate application to many problems of practical interest continues to provide a fascinating challenge for both theoretical and experimental work.

One of the simplest impact oscillators which can be studied analytically, comprises a periodically forced particle at a position $x(t)$ acting as a harmonic oscillator with an instantaneous impact against a fixed obstacle. For a model of the impact we consider Newton's law of restitution where the velocity of the particle reverses at each impact with a consequent loss of kinetic energy. This system is given by

$$\begin{array}{ll} \ddot{x}(t) + x(t) = f(t) & x(t) < \sigma, \\ \dot{x}(t^+) = -r\dot{x}(t^-) & x(t) = \sigma \end{array} \tag{1}$$

where $f(t)$ is a given periodic function, $0 \leq r \leq 1$ is the coefficient of restitution, σ is the clearance between the obstacle and the mean position of the oscillator and all derivatives are with respect to time. This model omits damping between impacts (see the papers by Chin *et. al.* [32] and Natsiavas [33] which include it), the reasons for which are twofold. Firstly, provided $r < 1$ the system above is dissipative and thus will have very similar dynamics to that with dissipation between impacts. The second reason is that the above system is much easier to analyse mathematically, and by looking for exact solutions of the motion we may obtain much insight into the more general case. The air bed experiments described in [23] show close agreement between the predictions of this model and the results of a practical demonstration. Furthermore, this simple model gives very good insights into the behaviour of the much more complicated system of the vibro-impacting cantilever beam Foale & Bishop [18], or an impacting cylindrical tube Goyda [3], both of which which oscillate in several modes and which have energy exchange between the modes at impact.

A very closely related impacting system to (1) comprises an unforced oscillator which impacts with and rebounds from a moving obstacle at a position $g(t)$. Thus

$$\begin{array}{rl} \ddot{y}(t)+y(t)=0, & y(t)>g(t) \\ \dot{y}(t^{+})=-r\dot{y}(t^{-})+(1+r)\dot{g}(t^{-}), & y(t)=g(t) \end{array} \tag{2}$$

To demonstrate the equivalence, [34] of the driven particle and driven obstacle models, we simply set

$$y(t)=a(t)-g(t), \quad \text{and} \quad f(t)=\ddot{g}(t)+g(t).$$

In the majority of both the analytic and experimental literature (see for example [35, 36, 37, 38, 39, 40, 41] and the references previously mentioned) the special case of periodic sinusoidal forcing has been considered for which

$$f(t)=\cos(\omega t), \tag{3}$$

and in this paper we extend this definition of $f(t)$ to the slightly more general periodic case of

$$f(t)=\cos(\omega t)+\alpha\cos(2\omega t), \tag{4}$$

which gives some insight into the most general periodic forcing described by a Fourier series. Two further generalisations we consider are replacing the linear oscillator in (1) by a forced nonlinear Duffing oscillator with damping. This is a simple example of an oscillator on a nonlinear spring. We also consider, briefly, the extension to (2) of including more than one impacting component.

The simplest forms of motion of the particle with periodic forcing are *periodic* motions which repeat after *one* impact. Such motions are mode-locked with the forcing and the time period between each (instantaneous) impact is given by

$$T=\frac{2\pi n}{\omega}, \quad n\in N. \tag{5}$$

In Budd *et. al.* [19] such orbits are referred to as $(1,n)$ orbits where the 1 describes the single impact between repeats. A similar classification is given in [37]. In Peterka such motion is referred to as a $z=1/n$ motion. With the forcing in (3) it is relatively easy to establish algebraic conditions for such orbits, see for example [13, 19, 35], although not all the orbits so calculated are physical and some involve penetrations of the obstacle between impacts. As a parameter, such as ω is varied these (physical) orbits typically lose stability through three mechanisms; namely saddle node bifurcations, period-doubling bifurcations and *grazing* bifurcations [4, 20, 32], where an intervening impact of zero velocity occurs between the existing impacts, or the velocity of one impact drops to zero. The first two bifurcations are relatively easy to analyse from local estimates but the third is much harder and involves global estimates of the flow. If ω is close to an even number, $2n$, then numerical simulations indicate strongly that the $(1,n)$ orbits are globally attracting, stable and have large amplitude with a well-pronounced resonant peak. Although we note that this peak changes substantially if the impact point is changed from being the equilibrium point of the oscillator, *i.e.* $\sigma\neq 0$. Such large amplitude motion may lead to high wear on the components of the system. It is for these reasons (and the ease of analysis) that has made a study of the $(1,n)$ orbits important. As ω is increased above $2n$ then a period-doubling bifurcation occurs at which the $(1,n)$ orbit loses stability to a $(2,2n)$ orbit, where the first 2 here refers to the two impacts between repeats. Further period–doubling and grazing bifurcations occur as ω is increased leading ultimately to an apparently chaotic motion. For larger values of ω, as $\omega \to 2(n+1)$, the chaotic motion vanishes and is replaced by a $(1, n+1)$ periodic motion.

In Figure 1 we present a bifurcation diagram of the solutions of (1), with the forcing given by (4) and $\sigma = 0,\ r = 0.8,\ \alpha = 0$ in which ω is increased from $\omega = 1.5$ to $\omega = 3.5$. The phase, $\phi = t_{\mathrm{mod} 2\pi/\omega}$ and velocity V of the impacts are plotted for 100 impacts of the recurrent motion of the particle after 3000 initial transients starting from the initial conditions $\phi_0 = 0.5,\ \dot{x}(\phi_0) = -1.5$.

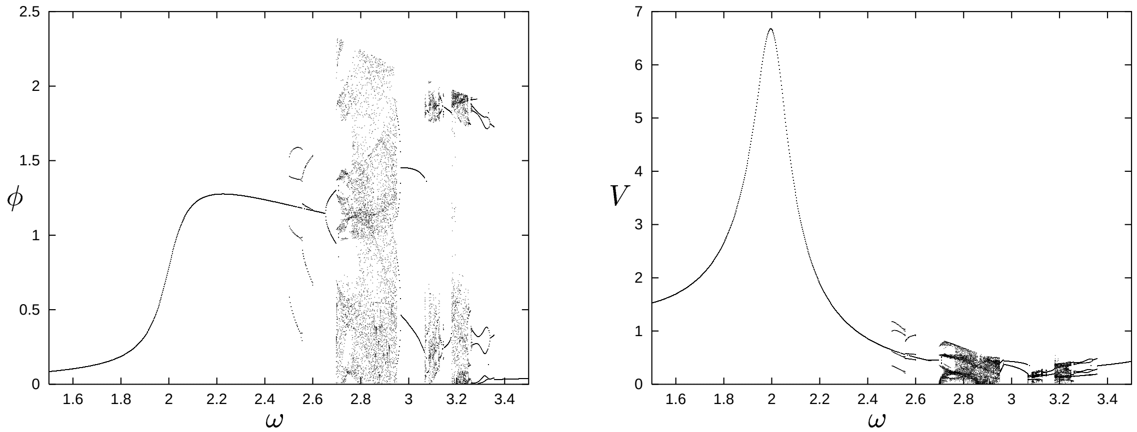

Figure 1: Bifurcation diagram showing impact phase (ϕ) and velocity (V) with $r = 0.8,\ \alpha = 0,\ \phi_0 = 0.5,\ \dot{x}(\phi_0) = -1.5$.

A very similar figure was obtained in the experiments reported in [23]. This figure displays two of the features we commented upon earlier. Firstly there is a large resonant $(1,1)$ periodic motion for $\omega \approx 2$ (which is repeated when $\omega \approx 4$) which period doubles to a $(2,2)$ periodic motion at about $\omega = 2.65$. Between $\omega \approx 2.7$ and $\omega \approx 3.35$ the motion is of low amplitude, generally complex and indeed appears to be chaotic for most of the parameter values. However, we observe that there is an interval centred upon $\omega = 3$ where the motion is of low amplitude and is a periodic $(2,2)$ orbit - having two impacts per period with period $T = 4\pi/3$. This motion seems to be stable and globally attracting. Indeed, an inspection of Figure 1 indicates that the $(2,2)$ orbit close to $\omega = 3$ is a re-emergence of the $(2,2)$ orbit created at the period-doubling bifurcation. The numerical experiments that we present in Section 6 show that when $\omega \approx 3$ a similar double impact periodic motion is observed in both the nonlinear Duffing oscillator and a system with more than one impacting component. Such double impact orbits occur in a neighbourhood of general odd values of ω such that if $\omega = 2n-1, n \in N$ there is an open interval of values of ω including this for which we see a $(2,n) = (2, (\omega+1)/2)$ orbit with period

$$T = \frac{2\pi n}{\omega} = \frac{\pi(\omega+1)}{\omega}. \tag{6}$$

We show further that if $\omega = 2n-1$ then there also exist families of $(2, 2n-1)$ orbits. These are non-physical (involving penetrations into the obstacle) when $\alpha = 0$ but exist for the forcing (4) even if $|\alpha|$ is quite small, and provided that r is close to one they are globally attracting.

From this observation of the existence and global stability of the two impact orbits for the odd values of ω we are motivated to study the existence and the stability of those orbits which have two impacts between repeats. Although motions more complex than the two-impact motion have been observed (see for example the paper [21] describing periodic motions with a very large number of impacts per period) the double impact motions seem to occur more often than any other forms of periodic motion, other than the single impact motions. The windows of existence around the odd integer values of ω help to explain this. Indeed, Reid & Whineray [23] found double impact motions in their experiments and expressed some surprise about the wide range of frequency values for which such behaviour was present.

Some early studies of such orbits were made by Kotera & Peterka [9] who wrote down the defining equations. These equations are far more complex than those for the $(1, n)$ periodic orbits, and in [9] a numerical approach was employed to study them and results reported for $r = 0.6, \omega = 0.92$ over a range of values of σ. A related numerical analysis of impacting systems with impacts between two obstacles have been reported in [13, 37].

The purpose of this present paper is to limit the investigation of these systems to the case when ω is close to an odd integer. When $\omega = 2n-1$ and $f(t)$ is given by (4), then the observed globally attracting $(2, n)$ and $(2, 2n-1)$ orbits can be written down in exact analytical form and we are able to make a detailed analysis of this case. For $\omega = 2n-1$ the stability and existence of these orbits then depends upon r and α and can be determined exactly. We can also see how these orbits change as ω, σ and α are varied and the defining system is generalised, although for this we must use a numerical approach.

The layout of this paper is as follows. In Section 2 we give a review of the general theory of impacting oscillators and of the related map P describing the motion from one impact to the next. In Section 3 we derive algebraic conditions for the existence and (linear) stability of the two-impact orbits. In Section 4 we determine the closed form solution of the two-impact orbits when $\omega = 2n-1$. In Section 5 we consider the stability and existence of the orbits as r, α and ω are varied and look at the persistence of these orbits as the mean point of the impact, σ changes. In particular, we look at conditions for the orbits we construct to be physical (i.e. avoiding penetrations of the obstacle) and demonstrate that the $(2, 2)$ orbit constructed when $\omega = 3$ is a natural continuation of the $(2, 2)$ orbit arising at a period-doubling bifurcation when $\omega = 2.65$. Finally in Section 6, we perform some numerical experiments to show that these results generalise to oscillators with a nonlinear restoring force and to oscillators with more than one impacting component. We also draw some conclusions from this work.

2 General Theory

If we consider the system (1) with an initial condition $x(t_0) = \sigma$ and $v(t_0) \equiv \dot{x}(t_0) \leq 0$, then a typical motion of the particle comprises a smooth flow, a discontinuous change in velocity at an impact followed by another smooth flow. Such a particle will then describe a trajectory $x(t)$. Because of the loss of energy at each impact the system is dissipative and all motion is ultimately on an absorbing set which contains an attractor - typically a periodic or a chaotic orbit. Details of the construction of this trajectory are described in [19]. This construction is not entirely straightforward as the particle may have an infinite number of impacts in a finite time and end up being stuck to the obstacle. However, these complications may be overcome provided that care is taken with the definition of the motion after sticking.

We now consider a trajectory for which the $i'th$. impact occurs at a time t_i with a positive velocity v_i *immediately before* the impact occurs. It is then shown by Whiston [35] (see also [19] for a more general development) that there is a well defined map P such that

$$P : (t_i, v_i) \to (t_{i+1}, v_{i+1}).$$

As the underlying forcing is periodic with period $2\pi/\omega$ we may exploit this to define a *phase*

$$\phi_i = (t_i)_{\mathrm{mod}(2\pi/\omega)}$$

so that

$$P : (\phi_i, v_i) \to (\phi_{i+1}, v_{i+1})$$

and P now acts on the cylinder with a coordinate discontinuity at $\phi = 2\pi/\omega$. The map P has interesting properties when either of the velocities v_i or v_{i+1} equal zero. In particular, the definition has to be carefully extended (due to sticking) when $v_i = 0$ and the map is *discontinuous* with infinite stretching when $v_{i+1} = 0$.

To construct P, using equation (4) as the forcing, we consider the trajectory $x(t) \equiv x(t; \sigma, -rv_0, t_0)$ with velocity $v(t) = dx/dt$ such that

$$x(t_0) = \sigma,$$

and

$$\dot{x}(t_0^-) \equiv v_0, \quad \dot{x}(t_0^+) \equiv -rv_0$$

are the respective velocities immediately before and after the impact at $t = t_0$. This trajectory is explicitly given by

$$x(t) = B\cos(t - t_0) + C\sin(t - t_0) + \gamma\cos(\omega t) + \alpha\delta\cos(2\omega t), \tag{7}$$

$$v(t) = C\cos(t - t_0) - B\sin(t - t_0) - \gamma\omega\sin(\omega t) - 2\alpha\delta\omega\sin(2\omega t), \tag{8}$$

where

$$B = \sigma - \gamma\cos(\omega t_0) - \alpha\delta\cos(2\omega t_0), \quad C = -rv_0 + \omega\gamma\sin(\omega t_0) + 2\alpha\delta\omega\sin(2\omega t_0),$$

$$\gamma = \frac{1}{1 - \omega^2}, \quad \text{and} \quad \delta = \frac{1}{1 - 4\omega^2}.$$

To compute P the first value $t = t_1 > t_0$ is determined such that

$$x(t_1; \sigma, -rv_0, t_0) = \sigma \tag{9}$$

and the corresponding value of v_1 evaluated. Whilst a closed form for P cannot be given explicitly, implicit differentiation of equation (9) gives an expression for the Jacobian derivative DP via the relations

$$\begin{aligned} \frac{\partial t_1}{\partial t_0} &= -\frac{1}{v_1}\frac{\partial x}{\partial t_0}\bigg|_{t=t_1}, & \frac{\partial t_1}{\partial v_0} &= -\frac{1}{v_1}\frac{\partial x}{\partial v_0}\bigg|_{t=t_1}, \\ \frac{\partial v_1}{\partial t_0} &= \frac{\partial v}{\partial t_0}\bigg|_{t=t_1} + \ddot{x}|_{x=\sigma}\frac{\partial t_1}{\partial t_0}, & \frac{\partial v_1}{\partial v_0} &= \frac{\partial v}{\partial v_0}\bigg|_{t=t_1} + \ddot{x}|_{x=\sigma}\frac{\partial t_1}{\partial v_0}. \end{aligned} \tag{10}$$

Thus

$$DP = \begin{pmatrix} \frac{1}{v1}\left(-rv_0c_{10} + A_0s_{10}\right) & -\frac{r}{v1}\left(s_{10}\right) \\ \left(-\left(A_0 + rA_1\frac{v_0}{v_1}\right)c_{10} - \left(rv_0 - \frac{A_0A_1}{v_1}\right)s_{10}\right) & -r\left(c_{10} - \frac{A_1}{v1}s_{10}\right) \end{pmatrix} \tag{11}$$

where $s_{10} = \sin(t_1 - t_0)$, $c_{10} = \cos(t_1 - t_0)$ and $A_0 = \cos(\omega t_0) + \alpha\cos(2\omega t_0) - \sigma$ and $A_1 = \cos(\omega t_1) + \alpha\cos(2\omega t_1) - \sigma$ are the accelerations at the two impacts. Thus $DP(r,\ v_0,\ v_1,\ t_0,\ t_1)$ is defined uniquely by (11).

Evaluation of the determinant of (11) gives

$$\det(DP) = r^2\frac{v_0}{v_1}. \tag{12}$$

We see from this expression that P has a well defined (invertible and differentiable) action on the phase space provided that $v_1 \neq 0$. If $v_1 = 0$ then P introduces (locally) infinite stretching to the phase space.

Note : It is shown in Lamba and Budd [22] that if P is considered to be the map from $(\phi, v^2) \to (\phi, v^2)$ then $\det(DP) = r^2$ and hence the map P is dissipative on this phase-space.

An (m, n) periodic orbit (also referred to by Peterka as an m/n orbit) is a trajectory which repeats after m impacts with a period of

$$T = \frac{2\pi n}{\omega}.$$

Such an orbit is necessarily a fixed point of the map P^m, the stability of which is (in general) governed by the eigenvalues of the corresponding Jacobian, although additional grazing instabilities occur when there is an intervening impact of zero velocity. In particular we can (in principle) observe periodic orbits for arbitrary values of m, although the cases of $m = 1, 2$ and 3 appear to be the most common. The case $m = \infty$ is also observed and refers either to a chaotic motion or a chattering motion in which an infinite number of impacts occurs in a finite time [21]. As remarked in the introduction, the vast majority of the existing analysis has been for $(1, n)$ orbits with $v_0 = v_1$ so that the necessary conditions for existence are simplified to finding v_0 and t_0. In particular, the time between impacts is known a-priori to be $2\pi n/\omega$. The algebraic conditions for the existence of these orbits also gives simple conditions for their linear stability. A complete analysis of the $(1,\ n)$ orbits and the impact map, P is given in [19].

3 Analysis of (2,n) orbits

A $(2, n)$ orbit may arise at a saddle-node bifurcation, a grazing bifurcation [4] or, in the special case of a $(2, 2k)$ orbit, at a period-doubling bifurcation from a $(1, k)$ orbit. It is periodic in time with period

$$T = \frac{2\pi n}{\omega}.$$

Such an orbit will typically have impacts at increasing times t_i, with $t_{i+2} = t_i + T$. The (smooth) flow between t_0 and t_1 is identical to the flow between t_2 and t_3 and we denote it by $x_0(t)$.

Similarly we denote the flow between t_1 and t_2 by $x_1(t)$. At each impact the restitution law applies so that

$$-r\dot{x}_0(t_1^-) = \dot{x}_1(t_1^+) \quad \text{and} \quad -r\dot{x}_1(t_2^-) = \dot{x}_0(t_2^+) = \dot{x}_0(t_0^+). \tag{13}$$

We define

$$v_0 = \dot{x}_1(t_0^-) = \dot{x}_1(t_2^-) \quad \text{and} \quad v_1 = \dot{x}_0(t_1^-)$$

to be the (positive) velocities immediately before each impact.

The analysis of the $(2, n)$ orbits is more difficult than for the $(1, n)$ orbits as the time of the intermediate impact t_1 is unknown and we need to solve four algebraic equations for four unknowns (as opposed to two for the single-impact orbits). However, we may easily apply the theory of the last section to each of the flows $x_0(t)$ and $x_1(t)$.

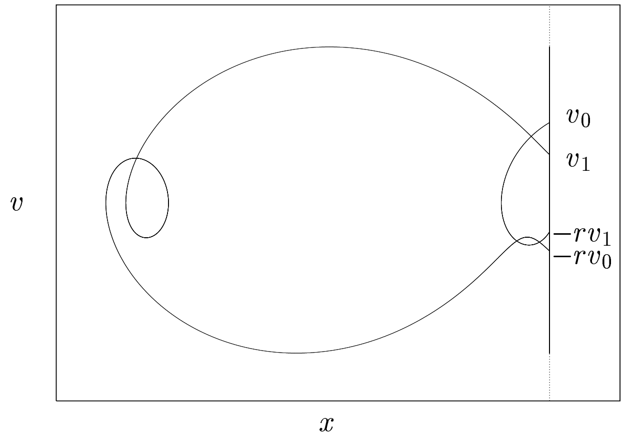

Figure 2: A schematic representation (in the phase plane) of a $(2, n)$ orbit.

For such a motion, see Figure 2, we have a first flow which impacts the obstacle at time t_1 with velocity $v = v_1$. There is then a second flow with initial velocity given by $v = -rv_1$. Extending (7),(8) we set

$$\begin{aligned} x_i(t) &= B_i \cos(t - t_i) + C_i \sin(t - t_i) + \gamma \cos(\omega t) + \alpha\delta \cos(2\omega t), \\ v_i(t) &= C_i \cos(t - t_i) - B_i \sin(t - t_i) - \omega\gamma \sin(\omega t) - 2\omega\alpha\delta \sin(2\omega t), \end{aligned} \qquad i = 0, 1. \tag{14}$$

Now using the conditions that

$$x_0(t_0) = x_0(t_1) = x_1(t_1) = x_1(t_2) = \sigma$$

and the relations (13) for the velocities of impact we have

$$\sigma = B_0 \cos(\Delta_{10}) + C_0 \sin(\Delta_{10}) + \gamma \cos(\omega t_1) + \alpha\delta \cos(2\omega t_1), \tag{15}$$

$$v_1 = C_0 \cos(\Delta_{10}) - B_0 \sin(\Delta_{10}) - \gamma\omega \sin(\omega t_1) - 2\alpha\delta\omega \sin(2\omega t_1), \tag{16}$$

$$\sigma = B_1 \cos(\Delta_{21}) + C_1 \sin(\Delta_{21}) + \gamma \cos(\omega t_2) + \alpha\delta \cos(2\omega t_2), \tag{17}$$

$$v_0 = C_1 \cos(\Delta_{21}) - B_1 \sin(\Delta_{21}) - \gamma\omega \sin(\omega t_2) - 2\alpha\delta\omega \sin(2\omega t_2), \tag{18}$$

where

$$B_0 = \sigma - \gamma \cos(\omega t_0) - \alpha\delta \cos(2\omega t_0), \quad C_0 = -rv_0 + \omega\gamma \sin(\omega t_0) + 2\alpha\delta\omega \sin(2\omega t_0),$$

$$B_1 = \sigma - \gamma\cos(\omega t_1) - \alpha\delta\cos(2\omega t_1), \quad C_1 = -rv_1 + \omega\gamma\sin(\omega t_1) + 2\alpha\delta\omega\sin(2\omega t_1),$$

$$\gamma = \frac{1}{1-\omega^2}, \quad \delta = \frac{1}{1-4\omega^2}$$

and

$$\Delta_{ij} = t_i - t_j, \quad \Delta_{10} + \Delta_{21} = T.$$

This is a system of four equations in the four unknowns t_0, Δ_{21}, v_0 and v_1 (where $\Delta_{10} = 2\pi n/\omega - \Delta_{21}$). A similar system is derived in [9]. It is significantly harder to solve than the related system of a single impact orbit for which the unknowns are only v_0 and t_0, with $\Delta_{10} = 2\pi n/\omega$ given explicitly. Indeed, this latter system can be reduced so that v_0 satisfies a simple quadratic equation with v_0 and σ lying on an ellipse [19]. No such simple reduction is available for the system above and the analysis has so far only been done for $(2, 2k)$ orbits very close to the period-doubling bifurcation point by Shaw and Holmes [12] or numerically by Kotera and Peterka [9].

The stability of the $(2, n)$ orbit can be determined by using implicit differentiation and using the expression (11). Such an orbit is (linearly) stable if all the eigenvalues of the Jacobian lie within the unit circle, and an unstable orbit has at least one eigenvalue outside the unit circle. As noted in Section 2, additional instabilities can occur if an (intermediate) impact of zero velocity takes place and a *grazing* bifurcation occurs.

For the case of $(2, n)$ orbits we compute the Jacobian of the full orbit by linearising over x_0 and x_1 in turn and taking the product of the resulting Jacobians. The Jacobian of the flow from the impact at time t_0 to that at t_1 is given by

$$DP_1 = \begin{pmatrix} \frac{1}{v_1}\left(-rv_0c_{10} + A_0s_{10}\right) & \frac{r}{v_1}\left(s_{10}\right) \\ \left(-\left(A_0 + rA_1\frac{v_0}{v_1}\right)c_{10} - \left(rv_0 - \frac{A_0A_1}{v_1}\right)s_{10}\right) & -r\left(c_{10} - \frac{A_1}{v_1}s_{10}\right) \end{pmatrix} \tag{19}$$

and for the second flow ($t_1 \to t_2$) by

$$DP_2 = \begin{pmatrix} \frac{1}{v_0}\left(-rv_1c_{21} + A_1s_{21}\right) & \frac{r}{v_0}\left(s_{21}\right) \\ \left(-\left(A_1 + rA_0\frac{v_1}{v_0}\right)c_{21} - \left(rv_1 - \frac{A_1A_0}{v_0}\right)s_{21}\right) & -r\left(c_{21} - \frac{A_0}{v_0}s_{21}\right) \end{pmatrix} \tag{20}$$

where $c_{ij} = \cos(\Delta_{ij})$, $s_{ij} = \sin(\Delta_{ij})$, $\Delta_{ij} = t_i - t_j$ and $i, j = 1, 0$ or $2, 1$ respectively. $A_i = \cos(\omega t_i) + \alpha\cos(2\omega t_i) - \sigma$, $i = 0, 1$ is the acceleration at the impacts. Hence the Jacobian for the $(2, n)$ orbit is given by the product of these.

In Section 5 we use this result to compute the stability of the explicitly calculated orbits in Section 4.

For completeness we now present a reduction of the four equations (15- 18). We reduce this system to two equations in the unknowns t_0 and Δ_{21}. A further reduction is possible [9] but the resulting equations are very complex and nonlinear and the two equation reduction is slightly clearer.

For a $(2, n)$ orbit, $t_2 = t_0 + 2n\pi/\omega$. Substituting this value into equations (15-18) we can eliminate the impact velocities. In particular, we can rearrange (17) to give an expression for v_1, which when substituted into (18) gives an expression for v_0. These take the form

$$
\begin{aligned}
v_1 = & - \frac{1}{r\sin(\Delta_{21})}\left(\sigma - (\sigma - \gamma\cos(\omega t_1) - \alpha\delta\cos(2\omega t_1))\cos(\Delta_{21}) - \gamma\cos(\omega t_0)\right. \\
& - \left.\alpha\delta\cos(2\omega t_0)\right) + \frac{1}{r}\left(\omega\gamma\sin(\omega t_1) + 2\alpha\omega\delta\sin(2\omega t_1)\right) \qquad (21)
\end{aligned}
$$

and

$$
\begin{aligned}
v_0 &= (v_1 + \omega\gamma\sin(\omega t_1) + 2\alpha\delta\omega\sin(2\omega t_1))\cos(\Delta_{21}) - (\sigma - \gamma\cos(\omega t_1) \\
&- \alpha\delta\cos(2\omega t_1))\sin(\Delta_{21}) - \gamma\omega\sin(\omega t_0) - 2\alpha\delta\omega\sin(2\omega t_0). \qquad (22)
\end{aligned}
$$

However, we now note that (21) (and therefore (22)) is indeterminate if $\Delta_{21} = k\pi,\ k \in N$. In order to overcome this problem we can similarly re-arrange equations (16) and (18) to get the following alternative expressions for v_0 and v_1

$$
\begin{aligned}
v_1 &= \left(\frac{r\cos(\Delta_{10})}{1 - r^2\cos(\Delta_{10})\cos(\Delta_{21})}\right)\left[\gamma\omega\left(\frac{1+r}{r}\right)\sin(\omega t_0) + 2\alpha\delta\omega\left(\frac{1+r}{r}\right)\sin(2\omega t_0)\right. \\
&- (\gamma\omega\sin(\omega t_1) + 2\alpha\delta\omega\sin(2\omega t_1))\left(\frac{1}{r\cos(\Delta_{10})} + \cos(\Delta_{21})\right) + (\sigma - \gamma\cos(\omega t_1) \\
&- \left.\alpha\delta\cos(2\omega t_1))\sin(\Delta_{21}) + (\sigma - \gamma\cos(\omega t_0) - \alpha\delta\cos(2\omega t_0))\left(\frac{\sin(\Delta_{10})}{r\cos(\Delta_{10})}\right)\right] \qquad (23)
\end{aligned}
$$

and

$$
\begin{aligned}
v_0 &= \left(\frac{r\cos(\Delta_{21})}{1 - r^2\cos(\Delta_{21})\cos(\Delta_{10})}\right)\left[\gamma\omega\left(\frac{1+r}{r}\right)\sin(\omega t_1) + 2\alpha\delta\omega\left(\frac{1+r}{r}\right)\sin(2\omega t_1)\right. \\
&- (\gamma\omega\sin(\omega t_0) + 2\alpha\delta\omega\sin(2\omega t_0))\left(\frac{1}{r\cos(\Delta_{21})} + \cos(\Delta_{10})\right) + (\sigma - \gamma\cos(\omega t_0) \\
&+ \left.\alpha\delta\cos(2\omega t_0))\sin(\Delta_{10}) - (\sigma - \gamma\cos(\omega t_1) - \alpha\delta\cos(2\omega t_1))\left(\frac{\sin(\Delta_{21})}{r\cos(\Delta_{21})}\right)\right]. \qquad (24)
\end{aligned}
$$

Now, (23) and (24) are also indeterminate but this time we require $\Delta_{21} = k\frac{\pi}{2},\ k \in N$ (we also note that (23) and (24) are indeterminate if $\cos(\Delta_{10})\cos(\Delta_{21}) = 1$ and $r = 1$).

We have now derived two sets (of two) equations describing the impact velocities v_0 and v_1. Substituting the first pair of equations (21,22) into (15) and (16), after some manipulation, yields the following two equations

$$
\begin{aligned}
A\gamma\cos(\omega t_0) + B\gamma\sin(\omega t_0) + C\alpha\delta\cos(2\omega t_0) + D\alpha\delta\sin(2\omega t_0) &= \sigma E, \\
F\gamma\cos(\omega t_0) + G\gamma\sin(\omega t_0) + H\alpha\delta\cos(2\omega t_0) + I\alpha\delta\sin(2\omega t_0) &= \sigma J,
\end{aligned} \qquad (25)
$$

and similarly substituting the second pair (23),24) into (15) and (17) yields another pair of equations given by

$$
\begin{aligned}
K\gamma\cos(\omega t_0) + L\gamma\sin(\omega t_0) + M\alpha\delta\cos(2\omega t_0) + N\alpha\delta\sin(2\omega t_0) &= \sigma O, \\
P\gamma\cos(\omega t_0) + Q\gamma\sin(\omega t_0) + R\alpha\delta\cos(2\omega t_0) + S\alpha\delta\sin(2\omega t_0) &= \sigma T,
\end{aligned} \qquad (26)
$$

where A to T are functions of Δ_{21}, $\Delta_{10}(= 2\pi n/\omega - \Delta_{21})$, r and ω, which can be found in Appendix A.

Thus, for given values of r, ω and n the above equations, (25) and (26), can be solved numerically to give t_0 and Δ_{21}. We have to use both equations (25) and (26) when searching for solutions because if we find $\Delta_{21} \to k\pi,\ k \in N$ when using equation (25) it becomes indeterminate (because of the equations governing the impact velocities, (21) and (22)). If this is the case, and $\Delta_{21} \to k\pi$ we simply change equations and carry on with the numerical technique, now using (26). The reverse is also true, where if we are using equation (26) and find $\Delta_{21} \to k\pi/2,\ k \in N$ again we simply change equations and carry on with a numerical method, now using (25). Thus, by using a combination of equations (25) and (26) we are able to find values of Δ_{21} and t_0 which correspond to $(2,\ n)$ orbits.

4 Some exact expressions for the $(2, n)$ orbits

It is clear from the previous section that the general analysis of the $(2, n)$ orbits is likely to be complicated. The transcendental equations (15-18) or (25,26) are hard to solve and it is very difficult to see the structure of the solutions. However, motivated by the numerical observations made in the introduction, we will examine the case of ω being an odd integer. As mentioned in the introduction, we can construct closed form expressions for the $(2, n)$ orbits in this case, and moreover, the orbits that we construct are precisely the globally attracting ones observed.

If $\omega = 3$ then there are distinct $(2, 2)$ and $(2, 3)$ double-impact orbits and we consider each of these in turn, looking at expressions for their form, their stability and (global) existence. The proof of our results works for general odd $\omega > 1$ but for clarity we present it for the special case of $\omega = 3$.

4.1 Analysis of the $(2, 2)$ orbits

Theorem 4.1 *If $\sigma = 0,\ \alpha = 0$ and $\omega = 3$ then there is a (2,2) periodic orbit such that*

$$x_0(t) = -\frac{1}{8}\sin(3\epsilon)\cos(t - t_0) + C_0 \sin(t - t_0) - \frac{1}{8}\cos(3t), \tag{27}$$

$$x_1(t) = \frac{1}{8}\sin(3\epsilon)\cos(t - t_1) + C_1 \sin(t - t_1) - \frac{1}{8}\cos(3t), \tag{28}$$

where

$$C_0 = \frac{\sqrt{3}}{8}\sin(3\epsilon), \quad C_1 = \frac{\sqrt{3}}{8r}\sin(3\epsilon) - \frac{3}{8r}(1 + r)\cos(3\epsilon).$$

$$\epsilon = \frac{1}{3}\tan^{-1}\left(\frac{\sqrt{3}(1 - r^2)}{1 + r^2}\right),$$

$$t_0 = -\frac{\pi}{6} - \epsilon, \quad t_1 = \frac{\pi}{6} - \epsilon$$

and

$$t_2 = \frac{4\pi}{3} - \frac{\pi}{6} - \epsilon.$$

Furthermore,

$$\Delta_{10} = \frac{\pi}{3} \quad \textit{and} \quad \Delta_{21} = \pi.$$

Proof

In the above statement of the theorem the appropriate coefficients B_0 and B_1 are given by

$$B_0 = -\frac{1}{8}\sin(3\epsilon), \quad \text{and} \quad B_1 = \frac{1}{8}\sin(3\epsilon).$$

After some manipulation it is possible to show that these satisfy the equations (15 - 18) directly when $\omega = 3$, but this does not give much indication as to how these results arise. To do this we make a systematic calculation of the coefficients. To calculate the coefficients of $\sin(t - t_i)$ and $\cos(t - t_i)$ we start with the general equations of motion of the impact oscillator given by (14) so that

$$x_i(t) = B_i \cos(t - t_i) + C_i \sin(t - t_i) - \frac{1}{8}\cos(3t) \tag{29}$$

$$\dot{x}_i(t) = C_i \cos(t - t_i) - B_i \sin(t - t_i) + \frac{3}{8}\sin(3t) \tag{30}$$

where we note that $\gamma = \frac{1}{1-\omega^2} = -\frac{1}{8}$ and the subscript i takes the values 0 or 1 corresponding to the particular flow.

We firstly consider $x_0(t)$ for $t_0 \le t \le t_1$. A simple calculation gives

$$x_0(t_0) \equiv 0 = B_0 - \frac{1}{8}\cos(3t_0)$$

and

$$x_0(t_1) \equiv 0 = B_0 \cos(\Delta_{10}) + C_0 \sin(\Delta_{10}) - \frac{1}{8}\cos(3t_1).$$

If we take

$$t_0 = -\frac{\pi}{6} - \epsilon, \quad t_1 = \frac{\pi}{6} + \epsilon \quad \text{and} \quad \Delta_{10} = \frac{\pi}{3}$$

we then have

$$B_0 = \frac{1}{8}\cos(3t_0) = -\frac{1}{8}\sin(3\epsilon) \quad \text{and} \quad C_0 = \frac{\sqrt{3}}{8}\sin(3\epsilon). \tag{31}$$

We now consider the flow $x_1(t)$. Again we have

$$x_1(t_1) \equiv 0 = B_1 - \frac{1}{8}\cos(3t_1)$$

which using the expression for t_1 gives

$$B_1 = \frac{1}{8}\sin(3\epsilon). \tag{32}$$

If we take $\Delta_{21} = \pi$ then we automatically have $x_1(t_2) = 0$ for this value of B_1 independent of the value of C_1.

It is here that we make explicit use of the fact that ω is odd. In one half cycle of the unforced oscillator we go though an odd number of half cycles of the forcing. Thus, an impact at time t_i guarantees an impact at $t_i + \pi$. This gives a major reduction in the complexity of the formulae and permits the construction of a simple analytic solution.

To determine the values of C_1 and ϵ we now consider the velocities of the impacts at the times t_0 and t_1. Considering first the impact at t_0. The velocity of $x(t)$ immediately before the impact at t_0 is given by

$$v_0 = \dot{x}_1(t_0^-) = x_1(t_2^+) = -B_1 \sin(\Delta_{21}) + C_1 \sin(\Delta_{21}) + \frac{3}{8}\sin(3t_0).$$

Thus if $\Delta_{21} = 4\pi/3 - \Delta_{10} = \pi$ we have

$$v_0 = -C_1 + \frac{3}{8}\sin(3t_2) = -C_1 - \frac{3}{8}\cos(3\epsilon).$$

Similarly, the velocity immediately after the impact is

$$-rv_0 = \frac{\sqrt{3}}{8}\sin(3\epsilon) - \frac{3}{8}\cos(3\epsilon).$$

Equating the two resulting expressions for v_0 we have (after some manipulation)

$$C_1 = \frac{\sqrt{3}}{8r}\sin(3\epsilon) - \frac{3}{8r}(1+r)\cos(3\epsilon). \tag{33}$$

Now we consider the impact at time t_1. The velocity immediately before this impact is given by

$$v_1 = \dot{x}_0(t_1^-) = -B_0 \sin(\Delta_{10}) + C_0 \cos(\Delta_{10}) + \frac{3}{8}\sin(3t_1) = -\frac{\sqrt{3}}{2}B_0 + \frac{1}{2}C_0 = \frac{3}{8}\sin(3t_1).$$

Furthermore, the velocity immediately after is given by

$$-rv_1 = \dot{x}_1(t_1^+) = C_1 + \frac{\sqrt{3}}{8}\sin(3t_1).$$

Equating these two expressions for v_1 and using the earlier expression for C_1 gives

$$\epsilon = \frac{1}{3}\tan^{-1}\left(\frac{\sqrt{3}(1-r^2)}{(1+r^2)}\right) \tag{34}$$

as required. $\square$

Corollary 4.2

The velocities at the impacts are

$$v_0 = \frac{3r}{8\sqrt{1-r^2+r^4}} \quad \textit{and} \quad v_1 = \frac{3}{8\sqrt{1-r^2+r^4}}. \tag{35}$$

We observe that as $r \to 1$, v_0 and v_1 both tend towards $\frac{3}{8}$ and $\epsilon \to 0$. In the limit of $r = 1$ we have

$$x_0(t) = -\frac{1}{8}\cos(3t), \quad x_1(t) = -\frac{3}{4}\sin(t - t_1) - \frac{1}{8}\cos(3t)$$

and

$$t_0 = -\frac{\pi}{6}, \quad t_1 = \frac{\pi}{6}, \quad t_2 = \frac{7\pi}{6}.$$

The motion $x_0(t)$ between t_0 and t_1 takes a particularly simple form and indeed is due to the forcing alone. For the driven obstacle problem (2) the function $y(t)$ is identically zero over such a time interval. This has certain interest in applications. For example it represents a minimum energy state of the particle, or for a more complex system (such as a cantilever beam) a state where the primary mode will have no significance and the effects of higher modes dominant.

This result can easily be extended to the case when ω is a general odd integer giving the following expression.

Theorem 4.3

If $\sigma = 0$ and $\alpha = 0$ then there is a $(2, \frac{1}{2}(1+\omega))$, $\omega \geq 3$ and odd, periodic orbit such that

$$x_0(t) = \gamma \sin(\omega\epsilon)\cos(t - t_0) + C_0 \sin(t - t_0) + \gamma\cos(\omega t), \tag{36}$$

$$x_1(t) = -\gamma \sin(\omega\epsilon)\cos(t - t_1) + C_1 \sin(t - t_1) + \gamma\cos(\omega t). \tag{37}$$

With

$$\epsilon = \frac{1}{\omega}\tan^{-1}\left(\frac{\omega s_\omega(1-r^2)}{(1+c_\omega)(1+r^2)}\right), \quad \gamma = \frac{1}{1-\omega^2},$$

$$C_0 = -\left(\frac{1+c_\omega}{s_\omega}\right)\gamma\sin(\omega\epsilon), \quad C_1 = -\left(\frac{1+c_\omega}{r s_\omega}\right)\gamma\sin(\omega\epsilon) + \frac{\gamma\omega}{r}(1+r)\cos(\omega\epsilon),$$

$$c_\omega = \cos\left(\frac{\pi}{\omega}\right), \quad s_\omega = \sin\left(\frac{\pi}{\omega}\right),$$

$$t_0 = -\frac{\pi}{2\omega} - \epsilon, \quad t_1 = \frac{\pi}{2\omega} - \epsilon.$$

Furthermore

$$\Delta_{10} = \pi/\omega \quad \textit{and} \quad \Delta_{21} = \pi.$$

Proof

This is similar to the proof of Theorem 4.1. Again, we take ω to be odd so that in one half cycle of the oscillator (during which $\Delta_{21} = \pi$) the forcing goes through precisely n-half cycles. It is this result which makes $x_1(t_2)$ independent of the value of C_1 and allows an easy calculation of ϵ and of C_1 without having to solve any transcendental equations. □

Although our exact result only applies for the special case of odd ω, the orbits so constructed perturb smoothly for a range of values of ω before becoming unstable. Interestingly, although the $(2, 2)$ orbit loses stability as ω is reduced, it re-stabilises again at a lower value of ω. This lower value of ω coincides with the $(2, 2)$ orbit arising from a period-doubling bifurcation of the $(1, 1)$ orbit as we increase ω from $\omega \approx 2$.

4.2 Analysis of the $(2, 3)$ orbits

Although our numerical experiments strongly indicate that the $(2, 2)$ orbit is the only globally attracting orbit when $\omega = 3, \sigma = 0$ and $\alpha = 0$ there are in fact two other double-impact periodic motions which exist for these parameters but are non-physical (as they involve penetrations of the obstacle). However, small changes to these parameters (in particular to α) gives two sets of physical $(2,3)$ orbits which also have a simple analytic form when $\omega = 3$. Unlike the $(2,2)$ orbit which had unequal times between impacts, these orbits have an equal time of π between each impact.

We now examine these orbits when $\omega = 3$ and then generalise our results to odd ω.

Theorem 4.4

If $\omega = 3$ and $|35\sigma/\alpha| < 1$ then there is a $(2,3)$ periodic orbit with coefficients B_i, C_i such that

$$B_0 = \frac{1}{8}\cos(3t_0), \quad B_1 = -\frac{1}{8}\cos(3t_0), \tag{38}$$

$$C_0 = -\frac{3}{8}\sin(3t_0) - \frac{6|\alpha|}{35}\sqrt{1 - \left(\frac{35\sigma}{\alpha}\right)^2}\left(\frac{1+r}{1-r}\right), \tag{39}$$

$$C_1 = \frac{3}{8}\sin(3t_0) - \frac{6|\alpha|}{35}\sqrt{1 - \left(\frac{35\sigma}{\alpha}\right)^2}\left(\frac{1+r}{1-r}\right), \tag{40}$$

where

$$t_0 = \frac{1}{6}\cos^{-1}\left(\frac{-35\sigma}{\alpha}\right), \quad t_1 = t_0 + \pi \tag{41}$$

and

$$\Delta_{10} = \Delta_{21} = \pi.$$

Here, the branch of $\cos^{-1}$ is taken such that

$$\alpha\sin(6t_0) > 0.$$

Proof

The proof of this result is simplified by the fact that the times between impacts of the two sub-orbits x_0 and x_1 are the same. Now

$$x_0(t) = B_0\cos(t - t_0) + C_0\sin(t - t_0) - \frac{1}{8}\cos(3t) - \frac{\alpha}{35}\cos(6t),$$

and if

$$-\frac{\alpha}{35}\cos(6t_0) = \sigma, \tag{42}$$

then $x_0(t_0) = \sigma$ provided $B_0 = \cos(3t_0)/8$. If we now take $t_1 = t_0 + \pi$ then as ω is odd we have $x_0(t_1) = \sigma$ and $\frac{\alpha}{35}\cos(6t_1) = \sigma$. Similarly, $x_1(t_1) = \sigma$ provided that $B_1 = \cos(3t_1)/8 = -B_0$. The velocity at the impact at t_1 is given by

$$v_1 = -C_0 + \frac{3}{8}\sin(3t_1) + \frac{6\alpha}{35}\sin(6t_1).$$

The identity (42) satisfied by t_0 is also satisfied by t_1 and hence

$$\alpha \sin(6t_1) = \alpha \sin(6t_1) = \pm\alpha\sqrt{1 - \left(\frac{35\sigma}{\alpha}\right)^2}.$$

Here the sign of the square root depends upon the branch of the function $\cos^{-1}$ used to evaluate t_0. Our future calculations, see (43) make it clear that for v_0 and v_1 to be positive we must choose the branch for which

$$\alpha \sin(6t_0) = |\alpha|\sqrt{1 - \left(\frac{35\sigma}{\alpha}\right)^2} > 0.$$

Evaluating the velocities at each impact we then have

$$v_1 = -C_0 - \frac{3}{8}\sin(3t_0) + \frac{6|\alpha|}{35}\sqrt{1 - \left(\frac{35\sigma}{\alpha}\right)^2},$$

$$-rv_0 = C_0 + \frac{3}{8}\sin(3t_0) + \frac{6|\alpha|}{35}\sqrt{1 - \left(\frac{35\sigma}{\alpha}\right)^2},$$

$$v_0 = -C_1 + \frac{3}{8}\sin(3t_0) + \frac{6|\alpha|}{35}\sqrt{1 - \left(\frac{35\sigma}{\alpha}\right)^2},$$

$$-rv_1 = C_1 - \frac{3}{8}\sin(3t_0) + \frac{6|\alpha|}{35}\sqrt{1 - \left(\frac{35\sigma}{\alpha}\right)^2}.$$

Equating these expressions gives the values of C_i stated in the theorem. $\square$

In Figure 3 we present a phase-plane plot of the $(2,3)$ orbit of Theorem 4.4, taking $\alpha = 0.5$.

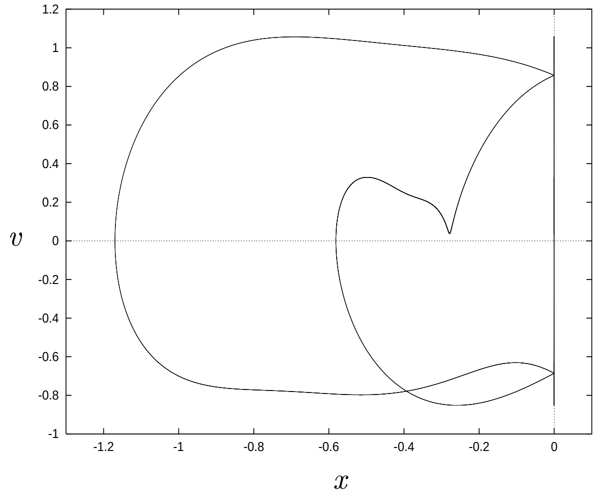

Figure 3: A $(2,3)$ orbit with $t_0 = \frac{\pi}{12}$, $t_1 = \frac{13\pi}{12}$ $\sigma = 0$, $r = 0.8$, $\omega = 3$ and $\alpha = 0.5$.

Corollary 4.5

For this orbit $v_0 = v_1$ *with*

$$v_0 = v_1 = \frac{12|\alpha|}{35(1-r)}\sqrt{1 - \left(\frac{35\sigma}{\alpha}\right)^2}. \tag{43}$$

Thus

- if α is fixed and $r \to 1$, both v_0 and $v_1 \to \infty$,
- if r is fixed and $\alpha \to 0$, both v_0 and $v_1 \to 0$.

Corollary 4.6

If $\sigma = 0$ then $t_0 = \pi/12$ if $\alpha > 0$ and $t_0 = \pi/4$ if $\alpha < 0$. Thus t_0 changes discontinuously as α passes through 0.

The result in Theorem 4.4 can be generalised to the case of general odd ω. In this case we have the following.

Theorem 4.7 *If $\omega \geq 3$ is odd and $|\sigma/(\alpha\delta)| < 1$ then there is a $(2, \omega)$ periodic orbit with coefficients*

$$B_0 = -\gamma\cos(t_0), B_1 = \gamma\cos(t_0) \tag{44}$$

$$C_0 = \omega\gamma\sin(\omega t_0) + 2\omega|\alpha|\delta\sqrt{1 - \left(\frac{\sigma}{\alpha\delta}\right)^2}\frac{1+r}{1-r}, \tag{45}$$

$$C_1 = -\omega\gamma\sin(\omega t_0) + 2\omega|\alpha|\delta\sqrt{1 - \left(\frac{\sigma}{\alpha\delta}\right)^2}\frac{1+r}{1-r}, \tag{46}$$

where

$$t_0 = \frac{1}{2\omega}\cos^{-1}\left(\frac{-\sigma}{\alpha\delta}\right), t_1 = t0 + \pi. \tag{47}$$

with

$$\gamma = \frac{1}{1-\omega^2}, \quad \textit{and} \quad \delta = \frac{1}{1-4\omega^2}. \tag{48}$$

Proof

This is a simple generalisation of the proof for $\omega = 3$. □

5 Linear stability and physicality of the double-impact orbits

For a solution of equations (15-18) to represent a physical orbit, two conditions must be satisfied namely

$$v_0 \quad \text{and} \quad v_1 \geq 0 \tag{49}$$

as well as

$$x(t) \leq \sigma \quad \text{for all} \quad t. \tag{50}$$

In general, as we vary a parameter, such as α, σ or ω there is a first value at which either (49) or (50) is violated and at which we have a grazing bifurcation leading to complex motion. We now consider the effect of varying each in turn.

5.1 Varying α

We have shown in the previous section that a $(2,2)$ orbit exists when $\alpha = 0$ and that a $(2,3)$ orbit exists for larger $|\alpha|$. Thus, as α is varied we expect there to be a transition from one form of orbit to the other. In Figure 4 three $(2,3)$ orbits are presented which were derived using Theorem 4.4 with $r = 0.8, \sigma = 0$ and $\omega = 3$. For $\alpha = 0.25$ the $(2,3)$ orbit penetrates the obstacle and (50) is violated. For $\alpha = 0.3$ it does not penetrate the obstacle and the $(2,3)$ orbit is therefore physical. The critical point at which penetration occurs and (50) is first violated is presented in the third figure and coincides with $\alpha = 0.2735$. For this value there is an intermediate impact of zero velocity. Thus, as α is decreased from a large positive value, the $(2,3)$ orbit will vanish, disappearing at a grazing bifurcation when $\alpha = 0.2735$. When α increases from a large negative value a grazing bifurcation occurs at $\alpha = -0.2815$.

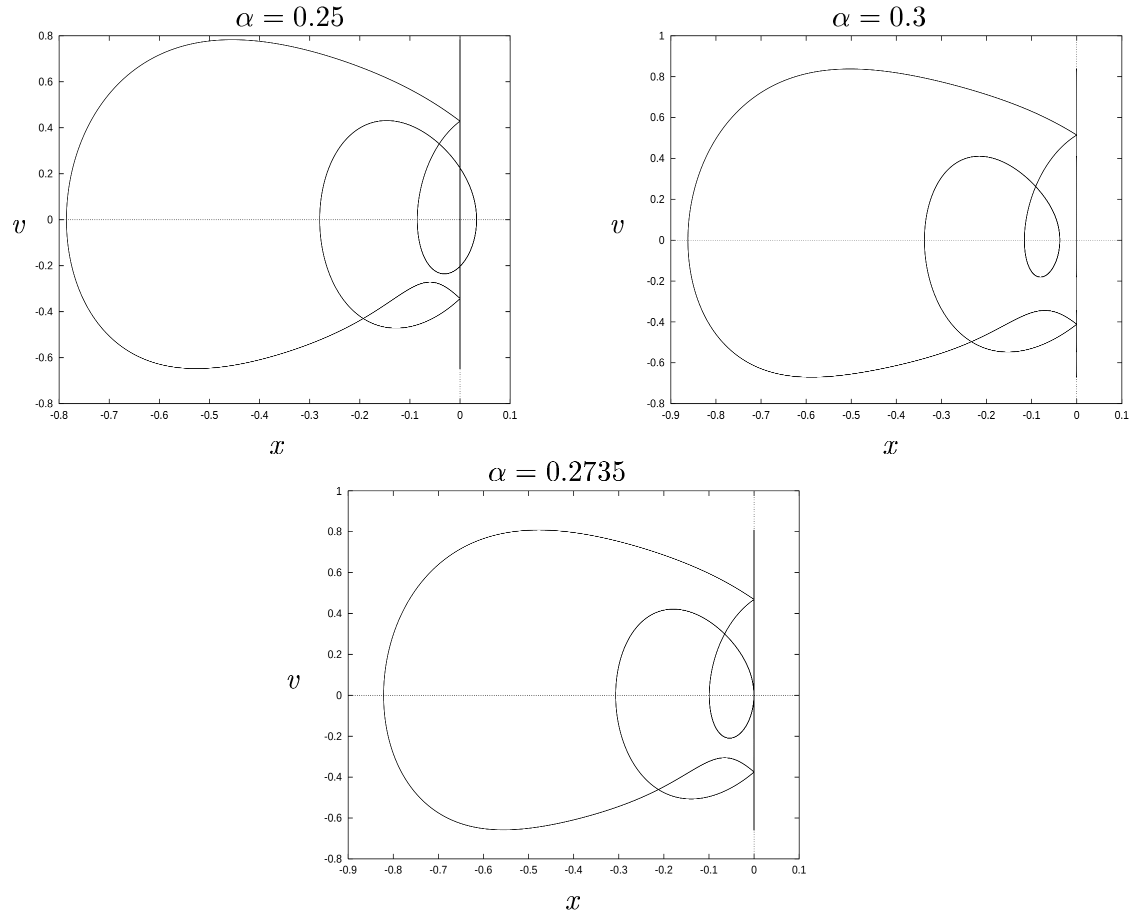

Figure 4: Three $(2,3)$ orbits with $t_0 = \frac{\pi}{12}$, $t_1 = \frac{13\pi}{12}$, $\sigma = 0$, $\omega = 3$ and $r = 0.8$.

In contrast, if we perturb $|\alpha|$ from zero with $\omega = 3, \sigma = 0$ and $r = 0.8$, the $(2,2)$ orbit exists for a small range of values and disappears at a period doubling bifurcation when $\alpha = 0.09$ and at a grazing bifurcation when $\alpha = -0.201$. There appear to be no values of α at which both the $(2,3)$ and $(2,2)$ orbits coexist. However, between $\alpha = -0.05$ and $\alpha = -0.52$ there is a complex (chaotic) motion which coexists with the $(2,2)$ and $(2,3)$ motions in turn. These results are illustrated by the bifurcation diagram presented in Figure 5.

In Table 1 we tabulate the values of both positive and negative α at which grazing bifurcations

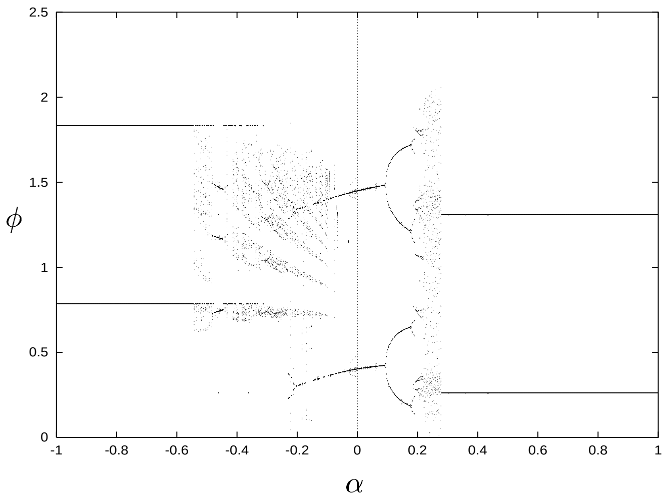

Figure 5: Bifurcation diagram showing impact phase (ϕ) for both negative and positive α with $r = 0.8,\ \omega = 3,\ \phi_0 = 0.5,\ \dot{x}(\phi_0) = -1.5$.

ω	3	5	7	9	11
α_+	0.2735	0.2642	0.2615	0.2610	0.2610
α_-	-0.2815	-0.2690	-0.2660	-0.2660	-0.2660

Table 1: Grazing bifurcation values for the $(2, \omega)$ orbits with $r = 0.8$.

occur for the $(2, 3)$ orbits for various ω when $r = 0.8$. We note from these values that as ω increases the *grazing* bifurcation points appear to be tending towards a constant value.

r	0.95	0.9	0.8	0.7	0.6
α_+	0.0638	0.1315	0.2735	0.4330	0.6120
α_-	-0.0643	-0.1325	-0.2815	-0.4520	-0.6465

Table 2: Grazing bifurcation values for the $(2, 3)$ orbits with $\omega = 3$.

Similarly, Table 2 presents the grazing bifurcation points arising when ω is fixed at $\omega = 3$ and r is varied. Here we note that as $r \to 1$ the *grazing* bifurcation values tend to zero, and we observe that the $(2, 3)$ orbit does not exist at $r = 1$ as v_0, v_1 are infinite in this limit.

5.2 Varying ω

Taking $r = 0.8$ we present in Figure 6 a bifurcation diagram with $\alpha = 0$ and varying ω. For values of ω close to 3 the $(2, 2)$ orbit perturbs smoothly, although it no longer has the nice analytic form described in Theorem 4.1. From this figure we see that when $r = 0.8$ the $(2, 2)$ orbit loses stability at a period doubling bifurcation when $\omega \approx 2.9675$ and as we decrease ω further chaotic motion occurs. As we increase ω above 3 the $(2, 2)$ orbit loses stability to chaotic motion at $\omega \approx 3.0855$ through a grazing bifurcation.

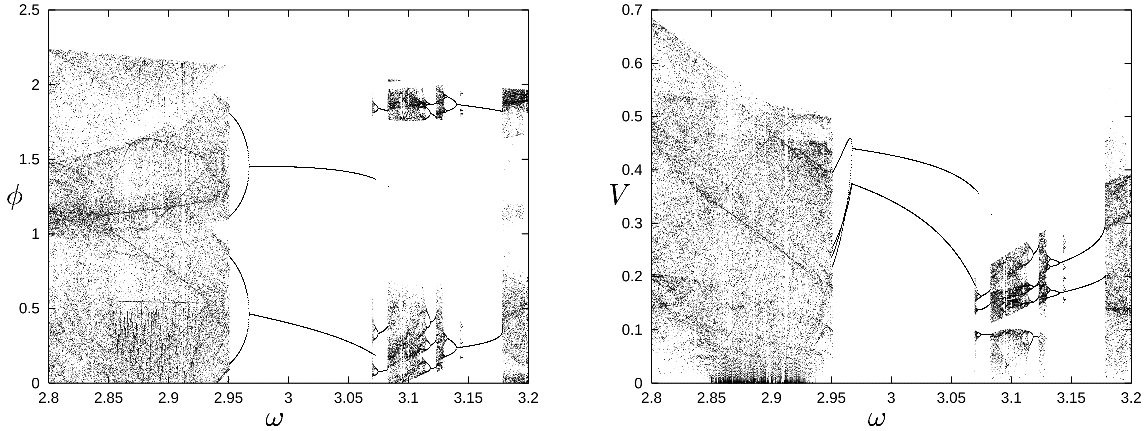

Figure 6: Bifurcation diagrams showing impact phase (ϕ) and velocity (V) with $\alpha = 0,\ r = 0.8,\ \sigma = 0,\ \phi_0 = 0.5$ and $\dot{x}(\phi_0) = -1.5$.

Varying r changes the value of ω at which the $(2,2)$ orbit loses stability through period-doubling or grazing bifurcations and we present values of these in Table 3.

r	0.95	0.8	0.65	0.61803
ω_{pd}	2.9625	2.9675	2.9900	3.0000
ω_g	3.0900	3.0855	3.0600	3.0500

Table 3: Period-doubling and grazing bifurcation values for the $(2,2)$ orbits.

It is most interesting to note, that although the $(2,2)$ orbit loses stability through a period-doubling bifurcation at $\omega \approx 2.9675$ it continues to exist (despite being unstable) as ω is reduced and becomes stable again for ω close to $\omega \approx 2.65$ where it coincides with the period-double of the $(1,1)$ orbit. To see this we present in Figure 7 a computation of the solutions governing this $(2,2)$ orbit as we reduce ω, using a simple continuation algorithm to follow the orbit. This behaviour is in contrast to that at a grazing bifurcation where the orbit is completely destroyed.

It is natural to ask whether similar behaviour is observed for ω close to another odd integer. Suppose for example that $\omega = 5$. The previous analysis would indicate that for suitable α either a $(2,3)$ or a $(2,5)$ orbit should exist in a neighbourhood of $\omega = 5$. Furthermore, for $\omega = 4$ there is a single (globally attracting) $(1,2)$ orbit which period doubles as ω is increased to a $(2,4)$ orbit. Such an orbit is quite distinct from the $(2,3)$ and $(2,5)$ orbits above and does not smoothly perturb into either as ω is increased to 5. In fact, when $\omega = 5, \alpha = 0$ and $\sigma = 0$ only the $(2,3)$ orbit is physical, and this orbit is also globally attracting.

5.3 Varying σ

Now, we consider the effect on the $(2,2)$ and $(2,3)$ orbits of varying the clearance, σ when $\omega = 3$. In Figure 8 we present two bifurcation diagrams with $r = 0.8,\ \omega = 3$ and α both zero and non-zero. Firstly setting $\alpha = 0$ we see that the $(2,2)$ orbit which exists when $\sigma = 0$, continues to exist in a neighbourhood of this value but loses stability when $|\sigma| \approx 0.1$ through a grazing

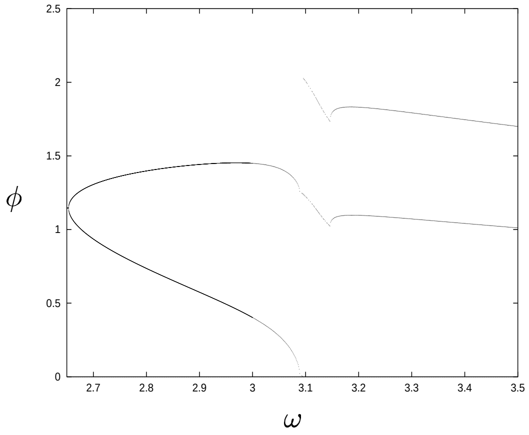

Figure 7: A diagram showing the $(2, 2)$ orbit as a function of ω. The orbit is unstable for $2.65 \leq \omega \leq 2.9675$ and non-physical for $\omega \geq 3.0855$.

bifurcation. For larger values of $|\sigma|$ we see only chaotic motion.

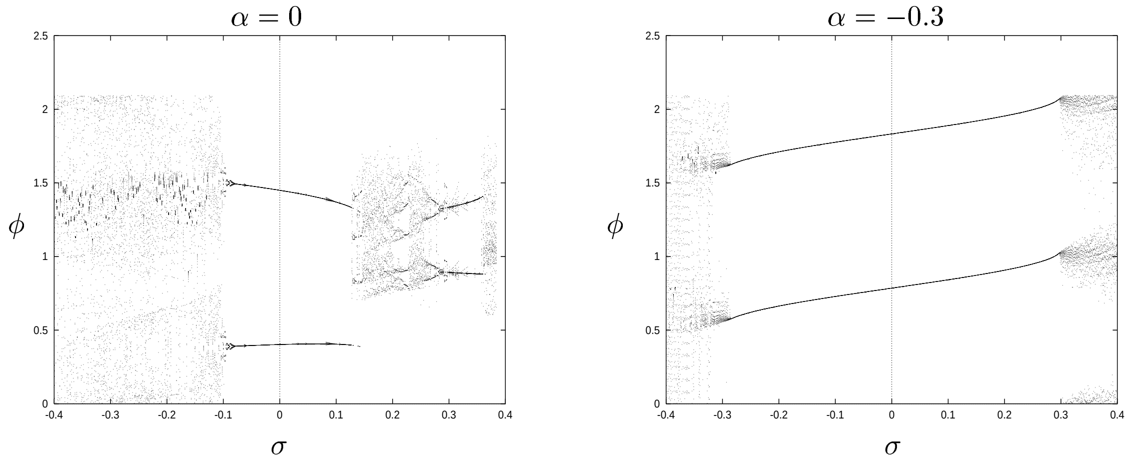

Figure 8: Bifurcation diagrams showing impact phase (ϕ) with $\alpha = 0$ and -0.3. Here $r = 0.8,\ \omega = 3,\ \phi_0 = 0.5$ and $\dot{x}(\phi_0) = -1.5$.

In the second figure we set $\alpha = -0.3$ and vary σ. In this case a $(2, 3)$ orbit exists when $\sigma = 0$ and persists for a greater range of the clearance, σ, than the $(2, 2)$ orbit shown in the first figure. However, the $(2, 3)$ orbit again loses stability at a grazing bifurcation when $35|\sigma| = |\alpha|$, which is precisely the condition for existence given in Theorem 4.4.

5.4 Linear stability analysis of the orbits

The (linear) stability of the $(2, 2)$ and $(2, 3)$ orbits can be examined analytically when $\omega = 3$ by evaluating the eigenvalues, $\lambda_{1,2}$ of the corresponding Jacobian, DP^2. This calculation is very straight forward given the exact analytic expressions for these orbits. For the $(2, 3)$ orbit, a simple calculation gives

$$\lambda_{1,2} = r^2, \quad r^2 \tag{51}$$

which are independent of α and σ. If $r < 1$ the eigenvalues lie within the unit circle and this orbit is linearly stable for all α. For $r = 1$ we have infinite impact velocities and the motion becomes unbounded.

A similar calculation shows that the eigenvalues for the $(2, \omega)$ orbit of Theorem 4.7 are also both equal to r^2 and hence these orbits are also linearly stable for all $r < 1$.

We now consider the $(2, 2)$ orbit constructed for $\alpha = 0$ in Theorem 4.1. In this case the eigenvalues $\lambda_{1,2}$, are given by the following expression

$$\lambda_{1,2} = \frac{1}{2}\left(3r^2 - 2 - 2r^4 \pm \sqrt{13r^4 - 12r^2 - 12r^6 + 4 + 4r^8}\right) \tag{52}$$

When $r > \frac{1}{\sqrt{2}}$ then $\lambda_{1,2}$ are complex, so that $|\lambda_{1,2}| = r^2 < 1$ and the orbit is stable. If we reduce r one eigenvalue passes through -1, and a period doubling bifurcation occurs where the $(2, 2)$ orbit loses stability to a $(4, 4)$ orbit.

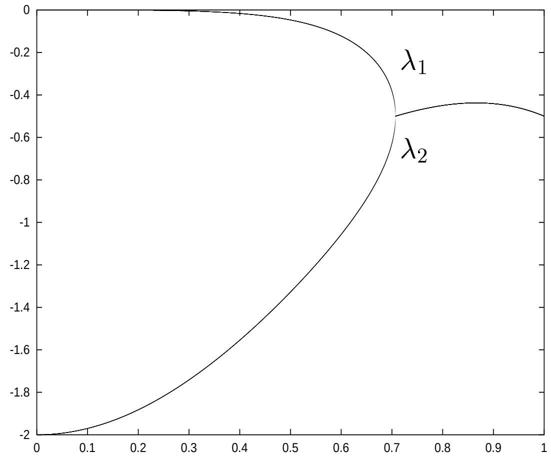

Figure 9: The real parts of the eigenvalues (as functions of r) for the $(2, 2)$ orbit.

The bifurcation point can be found analytically by solving the above equation for $\lambda_2 = -1$ which yields the following two equations

$$r^2 + r = 1 \quad \text{and} \quad r^2 - r = 1. \tag{53}$$

As we require the solution to be within the range $0 \leq r \leq 1$ we need only consider the first equation which gives

$$r = \psi \equiv \frac{1}{2}\left(\sqrt{5} - 1\right) \approx 0.61803. \tag{54}$$

Thus, the $(2, 2)$ orbit is linearly stable for $r > \psi$, and numerical calculations show that it is physical in this case. Similar behaviour is also observed for the $(2, \frac{1}{2}(1 + \omega))$ orbit and we note that the period doubling value, ψ increases as ω increases ($\psi_{\omega=5} \approx 0.764$).

We have already seen that when $\alpha = 0, r = 0.8$ and $\sigma = 0$ a period doubling bifurcation of the $(2, 2)$ orbit occurs when $\omega = 2.9675$. Similarly period doubling bifurcations occur when $\alpha = 0, r = \phi, \omega = 3$ and $\alpha = 0.1, r = 0.8, \omega = 3$. It is natural to infer from this that there exists a (two-dimensional) surface in the (α, r, ω) parameter space at which period-doubling bifurcations of the $(2, 2)$ orbit occur.

6 Generalisations and Conclusions

The analysis of the previous sections has been applied to the special case of the linear, single degree of freedom impact oscillator. It is important to ask, how well it carries over to more general examples of impacting oscillators. To see this we present some numerical calculations concerning two examples of generalisations, a nonlinear oscillator and an oscillator with more than one impacting component. Interestingly, although much of the dynamics of these oscillators differs from the simple model considered earlier, the double-impact motion at odd values of ω is very similar in both cases.

6.1 Example one: *The impacting Duffing oscillator*

For this example we look at an oscillator which comprises a forced mass moving with small damping on a cubically nonlinear softening spring, that impacts and rebounds from a fixed obstacle. Between impacts the oscillator satisfies the differential equation

$$\frac{d^2x}{dt^2} + \zeta \frac{dx}{dt} + F(x) = \cos(\omega t), \tag{55}$$

where

$$F(x) = x(t) - \gamma x(t)^3.$$

For large amplitude motions the nonlinearity is important, whereas for small amplitude motions it is less significant. In Figure 10 we present a bifurcation diagram of the attractor for this system when $\zeta = 0.01$ and $\gamma = 0.01$. This figure is directly comparable to Figure 1 for the undamped, linear oscillator. The addition of the nonlinearity clearly reduces the value of ω at which the main resonant peak occurs and introduces hysteresis into the bifurcation diagram. (Similar behaviour is, of course, observed in the smoothly forced Duffing oscillator without impact.)

In contrast, the motion around $\omega = 3$ is very similar to that of the linear oscillator. Indeed, double impact motion occurs for the Duffing oscillator for values of ω close to $\omega = 3$ and this motion closely resembles that of the linear oscillator. For example, it appears to arise at a period doubling bifurcation when $\omega \approx 2.8$ and persists (though unstable) throughout a chaotic band and finally disappears at a grazing bifurcation when $\omega \approx 3.1$. The reason for this similarity is simply that the low amplitude of the double-impact motion means that the effects of the nonlinearity of the oscillator are small and the exact double impact motion constructed in Section 4 for the linear oscillator perturbs smoothly to a double impact motion for the nonlinear oscillator. Similar behaviour will also occur for other nonlinear functions $F(x)$ provided that $F(x) \approx x$ when x is small.

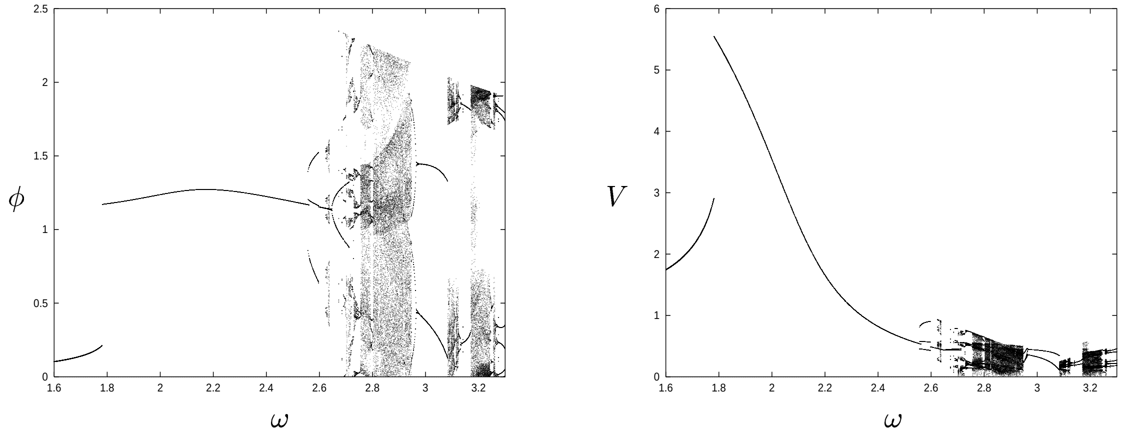

Figure 10: Bifurcation diagram showing impact phase (ϕ) and velocity (V) with $r = 0.8,\ \alpha = 0,\ \phi_0 = 0.5$ and $\dot{x}(\phi_0) = -1.5$.

6.2 Example two: *An impact oscillator with several oscillating components*

As a simple model for an impact oscillator with several components (for example the gears in a gear-box and the heat exchanger tubes in a nuclear reactor) we can consider a system of two oscillators coupled by impacts and forced by an impact with an oscillating wall. Such a system has the following form

$$\frac{d^2x}{dt^2} + x(t) = 0, \quad w(t) < x(t) \leq y(t) \tag{56}$$

$$\frac{d^2y}{dt^2} + y(t) = 0, \quad y(t) < x(t) \tag{57}$$

where

$$w(t) = \cos(\omega t).$$

For this system we consider $w(t)$ to be the location of an infinitely massive wall impacting with a particle at $x(t)$ which in turn impacts with a particle at $y(t)$. The law of impact is a generalisation of that given in (2) so that at a collision between $w(t)$ and $x(t)$ we have

$$\dot{x}(t^+) = -r\dot{x}(t^-) + (1+r)\dot{w}(t^-).$$

Similarly, at a collision between $x(t)$ and $y(t)$ we have

$$\dot{x}(t^+) = r(1-\epsilon)\left[\dot{y}(t^-) - \dot{x}(t^-)\right] + (1-\epsilon)\dot{y}(t^-) + \epsilon\dot{x}(t^-),$$

and

$$\dot{y}(t^+) = -r\epsilon\left[\dot{y}(t^-) - \dot{x}(t^-)\right] + \epsilon\dot{x}(t^-) + (1-\epsilon)\dot{y}(t^-),$$

where,

$$\epsilon = \frac{m_x}{m_x + m_y}, \quad 0 \leq \epsilon \leq 1$$

and m_x, m_y are the respective masses of the particles at $x(t)$ and $y(t)$. In Figure 11 we present four diagrams showing the phase and velocity of the two components $x(t)$ and $y(t)$ as ω varies, taking $\epsilon = 0.9$. Here we define

$$\phi_0 = t_0 \mathrm{mod}_{2\pi/\omega} \quad \text{and} \quad \phi_1 = t_1 \mathrm{mod}_{2\pi/\omega},$$

with

$$V_0 = \dot{x}(t_0) - \dot{w}(t_0) \quad \text{and} \quad V_1 = \dot{y}(t_1) - \dot{x}(t_1)$$

where t_0 corresponds to an impact between $w(t)$ and $x(t)$, and t_1 corresponds to an impact between $x(t)$ and $y(t)$.

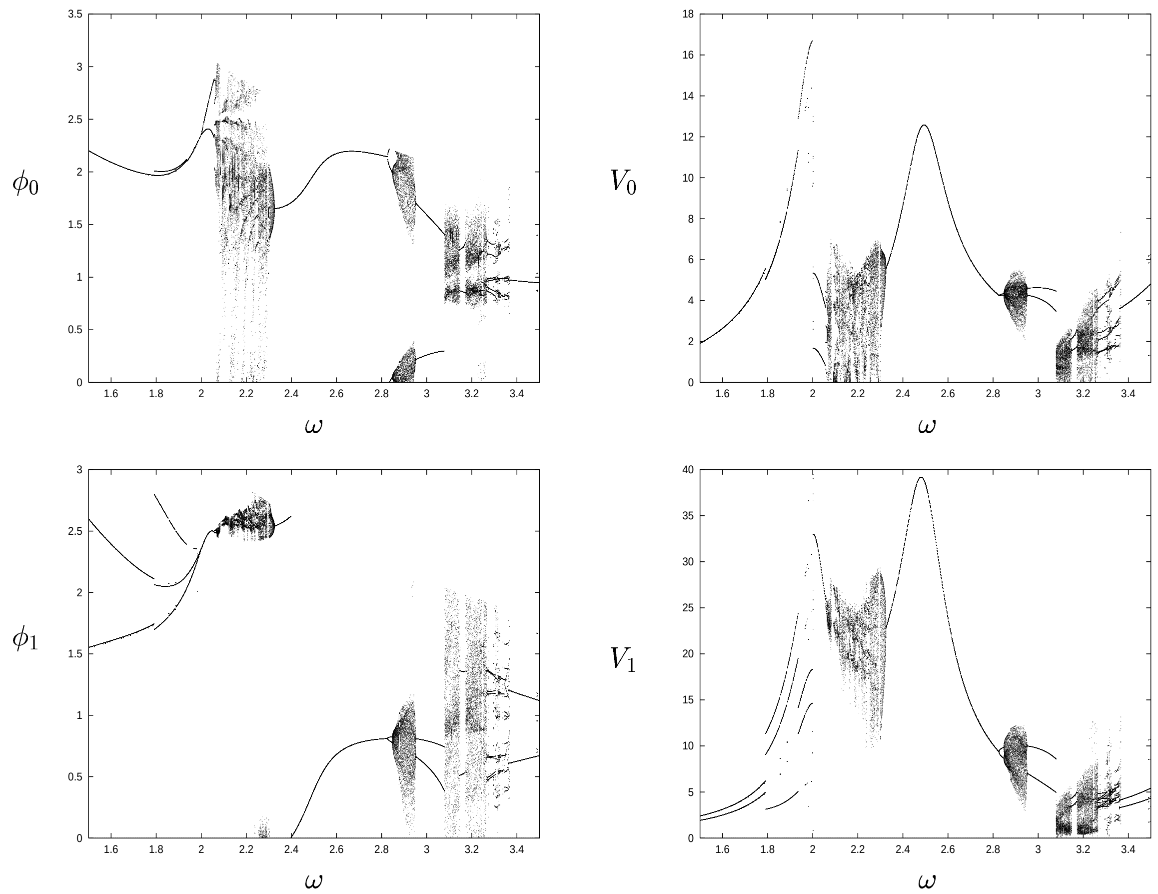

Figure 11: Bifurcation diagrams showing impact phases and velocities as functions of ω with $r = 0.8$ and $\epsilon = 0.9$.

The motion of this coupled system differs in many respects from that of the single degree of freedom impact oscillator. For example, there are now two pronounced resonant peaks at $\omega = 2$ and $\omega = 2.5$, and the behaviour of the second oscillator $y(t)$ is most complex if ω is slightly lower than the resonant value. A fuller discussion of this behaviour is made in [42]. However, despite all of this additional complexity, we note that if $\omega = 3$ then the whole motion simplifies again to a double impact periodic motion. Indeed, both of the two oscillators $x(t)$ and $y(t)$ exhibit the same form of motion. This double-impact orbit motion arises at a period doubling bifurcation when $\omega \approx 2.8$ and vanishes at a grazing bifurcation when $\omega \approx 3.1$ but is unstable for $2.81 \leq \omega \leq 3.95$. This calculation demonstrates that the the double impact motion arising when ω is odd generalises to systems with more degrees of freedom than the original.

In conclusion, this paper has described two simple forms of globally attracting double impact motion which arise when ω is close to an odd integer. These motions depend upon α, ω, σ and r and lose stability through period doubling or grazing bifurcations. Although it is only when ω is odd that we can give an exact expression for the orbits, the orbits so calculated appear to be stable to quite severe perturbations of the original problem and are thus highly likely to give an accurate description of the behaviour of a real (experimental) impact oscillator for these values of the forcing. We could also suggest that if such an oscillator is being controlled, then this represents a natural regime in which to operate it. This is because the double impact motion is both predictable and of low amplitude.

A The values of the coefficients in equations (25) and (26)

$$
\begin{aligned}
A &= \frac{1-\cos(\Delta_{21})}{r\sin(\Delta_{21})} - \omega\left(\frac{1}{r}+1\right)\sin(\omega\Delta_{21}) - \sin\left(\frac{2\pi n}{\omega}-\Delta_{21}\right) \qquad (58)\\
&- \cot\left(\frac{2\pi n}{\omega}-\Delta_{21}\right)\left(\cos\left(\frac{2\pi n}{\omega}-\Delta_{21}\right)-\cos(\omega\Delta_{21})\right),\\
B &= \cos(\omega\Delta_{21})\left(\frac{1}{r}+1\right) - \left(\frac{1}{r}\cot(\Delta_{21}) - \cot\left(\frac{2\pi n}{\omega}-\Delta_{21}\right)\right)\sin(\omega\Delta_{21}), \qquad (59)\\
C &= \frac{1}{r\sin(\Delta_{21})}\left(1-\cos(2\omega\Delta_{21})\cos(x)\right) - \frac{2\omega}{r}\sin(2\omega\Delta_{21}) - \sin\left(\frac{2\pi n}{\omega}-\Delta_{21}\right) \qquad (60)\\
&- \cot\left(\frac{2\pi n}{\omega}-\Delta_{21}\right)\left(\cos\left(\frac{2\pi n}{\omega}-\Delta_{21}\right)-\cos(2\omega\Delta_{21})\right),\\
D &= 2\omega\left(\frac{1}{r}+1\right)\cos(\omega\Delta_{21}) - \frac{\sin(2\omega\Delta_{21})\cos(\Delta_{21})}{r\sin(\Delta_{21})} - \cos\left(\frac{2\pi n}{\omega}-\Delta_{21}\right), \qquad (61)\\
E &= \frac{1-\cos(\Delta_{21})}{r\sin(\Delta_{21})} + \sin\left(\frac{2\pi n}{\omega}-\Delta_{21}\right)\cos\left(\frac{2\pi n}{\omega}-\Delta_{21}\right), \qquad (62)\\
F &= \left(\cos(\omega\Delta_{21})\cos(\Delta_{21})-1\right)\cot(\Delta_{21}) + \sin(\Delta_{21}) \qquad (63)\\
&- \frac{1}{r\sin\left(\frac{2\pi n}{\omega}-\Delta_{21}\right)}\left(1-\cos\left(\frac{2\pi n}{\omega}-\Delta_{21}\right)\right),\\
G &= \left(\frac{1}{r\sin\left(\frac{2\pi n}{\omega}-\Delta_{21}\right)} - \frac{1}{\sin(\Delta_{21})}\right)\sin(\omega\Delta_{21}) - 2\omega, \qquad (64)\\
H &= \left(\frac{1}{r\sin\left(\frac{2\pi n}{\omega}-\Delta_{21}\right)} - \frac{1}{\sin(\Delta_{21})}\right)\cos(2\omega\Delta_{21}) - \cot(\Delta_{21}) + \cot\left(\frac{2\pi n}{\omega}-\Delta_{21}\right), \qquad (65)\\
I &= -\left(\frac{1}{r\sin\left(\frac{2\pi n}{\omega}-\Delta_{21}\right)} + \frac{1}{\sin(\Delta_{21})}\right)\sin(2\omega\Delta_{21}) - 2(\omega+1), \qquad (66)\\
J &= \cot(\Delta_{21})\left(\cos(\Delta_{21})-1\right) - \frac{1}{r\sin\left(\frac{2\pi n}{\omega}-\Delta_{21}\right)}\left(1-\cos\left(\frac{2\pi n}{\omega}-\Delta_{21}\right)\right) + \sin(\Delta_{21}), \qquad (67)\\
K &= \left(\frac{-r^2\cos(\Delta_{21})\sin(\frac{2\pi n}{\omega}-\Delta_{21})}{1-r^2\cos(\frac{2\pi n}{\omega}-\Delta_{21})\cos(\Delta_{21})}\right)\left(\omega\left(\frac{1+r}{r}\right)\sin(2\pi n-\omega\Delta_{21})\right.\\
&+ \left.\cos(2\pi n-\omega\Delta_{21})\frac{\sin(\Delta_{21})}{r\cos(\Delta_{21})} - \sin(\frac{2\pi n}{\omega}-\Delta_{21})\right) + \cos(2\pi n-\omega\Delta_{21})\\
&- \cos(\frac{2\pi n}{\omega}-\Delta_{21}), \qquad (68)\\
L &= \left(\frac{-r^2\cos(\Delta_{21})\sin(\frac{2\pi n}{\omega}-\Delta_{21})}{1-r^2\cos(\frac{2\pi n}{\omega}-\Delta_{21})\cos(\Delta_{21})}\right)\left(\omega\left(\frac{1+r}{r}\right)\cos(2\pi n-\omega\Delta_{21})\right.\\
&- \left.\omega\left(cos(\frac{2\pi n}{\omega}-\Delta_{21}) + \frac{1}{r\cos(\Delta_{21})}\right) - \sin(2\pi n-\omega\Delta_{21})\frac{\sin(\Delta_{21})}{r\cos(\Delta_{21})}\right)\\
&- \sin(2\pi n-\omega\Delta_{21}) + \omega\sin(\frac{2\pi n}{\omega}-\Delta_{21}), \qquad (69)\\
M &= \left(\frac{-r^2\cos(\Delta_{21})\sin(\frac{2\pi n}{\omega}-\Delta_{21})}{1-r^2\cos(\frac{2\pi n}{\omega}-\Delta_{21})\cos(\Delta_{21})}\right)\left(2\omega\left(\frac{1+r}{r}\right)\sin(4\pi n-2\omega\Delta_{21})\right.
\end{aligned}
$$

$$
\begin{aligned}
&+ \quad \cos(4\pi n - 2\omega\Delta_{21})\frac{\sin(\Delta_{21})}{r\cos(\Delta_{21})} - \sin(\frac{2\pi n}{\omega} - \Delta_{21})\Big) + \cos(4\pi n - 2\omega\Delta_{21}) \\
&- \quad \cos(\frac{2\pi n}{\omega} - \Delta_{21}), \qquad (70)
\end{aligned}
$$

$$
\begin{aligned}
N &= \left(\frac{-r^2\cos(\Delta_{21})\sin(\frac{2\pi n}{\omega} - \Delta_{21})}{1 - r^2\cos(\frac{2\pi n}{\omega} - \Delta_{21})\cos(\Delta_{21})}\right)\left(2\omega\left(\frac{1+r}{r}\right)\cos(4\pi n - 2\omega\Delta_{21})\right. \\
&- 2\omega\left(cos(\frac{2\pi n}{\omega} - \Delta_{21}) + \frac{1}{r\cos(\Delta_{21})}\right) - \sin(4\pi n - 2\omega\Delta_{21})\frac{\sin(\Delta_{21})}{r\cos(\Delta_{21})}\Big) \\
&- \sin(4\pi n - 2\omega\Delta_{21}) + 2\omega\sin(\frac{2\pi n}{\omega} - \Delta_{21}), \qquad (71)
\end{aligned}
$$

$$
\begin{aligned}
O &= 1 - \left(\frac{-r^2\cos(\Delta_{21})\sin(\frac{2\pi n}{\omega} - \Delta_{21})}{1 - r^2\cos(\frac{2\pi n}{\omega} - \Delta_{21})\cos(\Delta_{21})}\right)\left(\sin(\frac{2\pi n}{\omega} - \Delta_{21}) - \frac{\sin(\Delta_{21})}{r\cos(\Delta_{21})}\right) \\
&- \cos(\frac{2\pi n}{\omega} - \Delta_{21}), \qquad (72)
\end{aligned}
$$

$$
\begin{aligned}
P &= \left(\frac{-r^2\cos(\Delta_{21})\sin(\frac{2\pi n}{\omega} - \Delta_{21})}{1 - r^2\cos(\frac{2\pi n}{\omega} - \Delta_{21})\cos(\Delta_{21})}\right)\left(\frac{\sin(\frac{2\pi n}{\omega} - \Delta_{21})}{r\cos(\frac{2\pi n}{\omega} - \Delta_{21})} - \omega\sin(2\pi n - \omega\Delta_{21})\left(\cos(\Delta_{21})\right.\right. \\
&+ \left.\frac{1}{r\cos(\frac{2\pi n}{\omega} - \Delta_{21})}\right) - \cos(2\pi n - \omega\Delta_{21})\sin(\Delta_{21})\Big) - \cos(2\pi n - \omega\Delta_{21})\cos(\Delta_{21}) \\
&+ \sin(\Delta_{21})\omega\sin(2\pi n - \omega\Delta_{21}) + 1, \qquad (73)
\end{aligned}
$$

$$
\begin{aligned}
Q &= \left(\frac{-r^2\cos(\Delta_{21})\sin(\frac{2\pi n}{\omega} - \Delta_{21})}{1 - r^2\cos(\frac{2\pi n}{\omega} - \Delta_{21})\cos(\Delta_{21})}\right)\left(\omega\frac{1+r}{r} - \omega\cos(2\pi n - \omega\Delta_{21})\left(\cos(\Delta_{21})\right.\right. \\
&+ \left.\frac{1}{r\cos(\frac{2\pi n}{\omega} - \Delta_{21})}\right) + \sin(2\pi n - \omega\Delta_{21})\sin(\Delta_{21})\Big) + \sin(2\pi n - \omega\Delta_{21})\cos(\Delta_{21}) \\
&+ \omega\cos(2\pi n - \omega\Delta_{21})\sin(\Delta_{21}), \qquad (74)
\end{aligned}
$$

$$
\begin{aligned}
R &= \left(\frac{-r^2\cos(\Delta_{21})\sin(\frac{2\pi n}{\omega} - \Delta_{21})}{1 - r^2\cos(\frac{2\pi n}{\omega} - \Delta_{21})\cos(\Delta_{21})}\right)\left(\frac{\sin(\frac{2\pi n}{\omega} - \Delta_{21})}{r\cos(\frac{2\pi n}{\omega} - \Delta_{21})} - 2\omega\sin(2\pi n - \omega\Delta_{21})\left(\cos(\Delta_{21})\right.\right. \\
&+ \left.\frac{1}{r\cos(\frac{2\pi n}{\omega} - \Delta_{21})}\right) - \cos(4\pi n - 2\omega\Delta_{21})\sin(\Delta_{21})\Big) - \cos(4\pi n - 2\omega\Delta_{21})\cos(\Delta_{21}) \\
&+ 2\omega\sin(\Delta_{21})\sin(2\pi n - \omega\Delta_{21}) + 1, \qquad (75)
\end{aligned}
$$

$$
\begin{aligned}
S &= \left(\frac{-r^2\cos(\Delta_{21})\sin(\frac{2\pi n}{\omega} - \Delta_{21})}{1 - r^2\cos(\frac{2\pi n}{\omega} - \Delta_{21})\cos(\Delta_{21})}\right)\left(2\omega\frac{1+r}{r} - 2\omega\cos(4\pi n - 2\omega\Delta_{21})\left(\cos(\Delta_{21})\right.\right. \\
&+ \left.\frac{1}{r\cos(\frac{2\pi n}{\omega} - \Delta_{21})}\right) + \sin(4\pi n - 2\omega\Delta_{21})\sin(\Delta_{21})\Big) + \sin(4\pi n - 2\omega\Delta_{21})\cos(\Delta_{21}) \\
&+ 2\omega\cos(4\pi n - 2\omega\Delta_{21})\sin(\Delta_{21}), \qquad (76)
\end{aligned}
$$

$$
T = 1 - \left(\frac{-r^2\cos(\Delta_{21})\sin(\frac{2\pi n}{\omega} - \Delta_{21})}{1 - r^2\cos(\frac{2\pi n}{\omega} - \Delta_{21})\cos(\Delta_{21})}\right)\left(\sin(\Delta_{21}) - \frac{\sin(\frac{2\pi n}{\omega} - \Delta_{21})}{r\cos(\frac{2\pi n}{\omega} - \Delta_{21})}\right) - \cos(\Delta_{21}). \qquad (77)
$$

Acknowledgements

The authors would like to thank Dr. H. Lamba for many helpful discussions and for his comments on the text. AGL would also like to thank the EPSRC for their financial support through an Earmarked studentship.

References

[1] A. Kaharaman and R. Singh. Nonlinear dynamics of a spur gear pair. *J. Sound Vib.*, 142:49–75, 1990.

[2] SH. Doole and SJ. Hogan. The nonlinear dynamics of suspension bridges under harmonic forcing. *Proc. Roy. Soc. Lond. A*, submitted.

[3] H. Goyda and C. Teh. A study of the impact dynamics of loosley supported heat exchanger tubes. *ASME Journal of Pressure Technology*, 111:394–401, 1989.

[4] AB. Nordmark. Non-periodic motion caused by grazing incidence in an impact oscillator. *J. Sound Vib.*, 145(2):279–297, 1991.

[5] F. Peterka and J. Vacik. Transition to chaotic motion in mechanical systems with impacts. *J. Sound Vib.*, 154(1):95–115, 1992.

[6] F. Peterka. Part 1 : Theoritical analysis of n-multiple (1/n)-impact solutions. *CSAV Acta Technica*, 19(4):462–473, 1974.

[7] F. Peterka. Part 2 : Results of analogue computer modelling of the motion. *CSAV Acta Technica*, 19(5):569–580, 1974.

[8] F. Peterka and J. Vacik. Part 3 : Stastical characteristics of beat motions. *CSAV Acta Technica*, 26(2):161–184, 1981.

[9] T. Kotera and F. Peterka. Part 4 : Analytical solution of the 2/n-impact motions and its stability. *CSAV Acta Technica*, 26(6):747–758, 1981.

[10] F. Peterka and T. Kotera. Part 5 : Regions of existence and stability and domains of attraction of different kinds of impact motion. *CSAV Acta Technica*, 27(1):92–117, 1982.

[11] T. Kotera and F. Peterka. Part 6 : Analytical and analogue solution of the multiple-impact motion and its stability. *CSAV Acta Technica*, 29(3):255–279, 1984.

[12] SW. Shaw and PJ. Holmes. A periodically forced piecewise linear oscillator. *J. Sound Vib.*, 90(1):129–155, 1983.

[13] SW. Shaw. The dynamcis of a harmonically excited system having rigid amplitude constraints. part 1 : Subharmonic motions and local bifurcations. *Journal of Applied Mechanics*, 453:453–458, 1985.

[14] SW. Shaw. The dynamcis of a harmonically excited system having rigid amplitude constraints. part 2 : Chaotic motions and global bifurcations. *Journal of Applied Mechanics*, 453:459–464, 1985.

[15] SW. Shaw. Forced vibrations of a beam with one-sided amplitude constraint: Theory and experiment. *J. Sound Vib.*, 99(2):199–212, 1985.

[16] JMT. Thompson and H. Stewart. *Nonlinear Dynamics and chaos.* New York : John Wiley, 1986.

[17] S. Foale and SR. Bishop. Dynamical complexities of forced impacting systems. *Phil. Trans. Roy. Soc. Lond A*, 338:547–556, 1992.

[18] S. Foale and SR. Bishop. *Bifurcations in Impact Oscillators : theory and expermiment. In Proc. IUTAM Symp. Nonlinear Dynamics Chaos engng Dynamics.* Wiley, 1994.

[19] CJ. Budd, FJ. Dux, and KA. Cliffe. The effect of frequency and clearance variations on a single degree of freedom impact oscillator. *J. Sound Vib.*, to appear.

[20] CJ. Budd and FJ. Dux. Intermittency in impact oscillators close to resonance. *Nonlinearity*, 7:1191–1124, 1994.

[21] CJ. Budd and FJ. Dux. Chattering and related behaviour in impact oscillators. *Phil. Trans. R. Soc. A*, 347:365–389, 1994.

[22] H. Lamba and CJ. Budd. Scaling of lyapunov exponents at non-smooth bifurcations. *Physical Review E*, 50:84–91, 1994.

[23] C. Reid and S. Whineray. The resonant response of a simple harmonic half-oscillator. *Phys. Lett. A*, 199:89–105, 1995.

[24] M. Sharkady J. Cusumano and B. Kimble. Experimental measurements of dimensionality and spatial coherence in the dynamics of a flexible beam impact oscillator. *Phil. Trans. Roy. Soc. Lond A*, 347:421–438, 1994.

[25] T. Mullin. Experimental observations of vibro-impact in a cantilever beam. *In preparation*, 1995.

[26] K. Popp. Regelung eines technischen prozesses mit pearl. *Insiitut fur Regelungstechnik, Universitat Hannover report*, 1995.

[27] K. Popp and P. Stelter. *Nonlinear oscillations of structures induced by dry friction, in Nonlinear Dynamics in Engineering Systems-IUTEM Symposium Stuttgart.* Springer, 1989.

[28] K. Popp and P. Stelter. Stick-slip vibrations and chaos. *Phil. Trans. Roy. Soc. Lond A*, 332:89–105, 1990.

[29] J. Deane D. Hamil and D. Jeffries. Modelling of chaotic dc-dc converters using iterated nonlinear mappings. *IEEE trans. on Power Electronics*, 7:25–36, 1992.

[30] F. Pfeiffer and M. Hajek. Stick-slip motions of turbine blade dampers. *Phil. Trans. Roy. Soc. Lond A*, 338:503–517, 1992.

[31] H. Lamba. *Impacting oscillators and non-smooth dynamical systems.* PhD thesis, University of Bristol, December 1993.

[32] W. Chin, E. Ott, HE. Nusse, and C. Grebogi. Grazing bifurcations in impact oscillators. *Physical Review E*, 50(6):4427–4444, 1994.

[33] S. Natsiavas. On the dynamics of oscillators with bi-linear damping and stiffness. *Int. J. Non-Linear Mechanics*, 25(5):535–554, 1990.

[34] H. Lamba. Chaotic, regular and unbounded behaviour in the elastic impact oscillator. *Physica D*, 82:117–135, 1995.

[35] GS. Whiston. The vibro-impact response of a harmonically excited and preloaded one-dimensional linear oscillator. *J. Sound Vib.*, 115:303–324, 1987.

[36] S. Natsiavas. Dynamics of multiple-degree-of-freedom oscillators with colliding components. *J. Sound Vib.*, 165(3):439–453, 1992.

[37] SJ. Hogan. On the dynamics of rigid-block motion under harmonic forcing. *Proc. R. Soc. Lond.*, 425(A):441–476, 1989.

[38] SJ. Hogan. Hetroclinic bifurcations in damped rigid block motion. *Proc. R. Soc. Lond.*, 439:155–162, 1992.

[39] S. Natsiavas. Stability and bifurcation analysis for oscillators with motion limiting constraints. *J. Sound Vib.*, 141(1):97–102, 1990.

[40] B. Feeny and FC. Moon. Chaos in a forced dry-friction oscillator : Experiments and numerical modelling. *J. Sound Vib.*, 170(3):303–323, 1994.

[41] GX. Li, RH. Rand, and FC.Moon. Bifurations and chaos in a forced zero-stiffness impact oscillator. *Int. J. Non-Linear Mechanics*, 25(4):417–432, 1990.

[42] AG. Lee. The behaviour of a row of impact oscillators. *In preparation*, 1995.